EUROFUSION WPS1-CP(16) 15150

D Moseev et al.

Application of the ECRH radiation for plasma diagnostics in Wendelstein 7-X

Preprint of Paper to be submitted for publication in
Proceedings of 26th IAEA Fusion Energy Conference

This work has been carried out within the framework of the EUROfusion Consortium and has received funding from the Euratom research and training programme 2014-2018 under grant agreement No 633053. The views and opinions expressed herein do not necessarily reflect those of the European Commission.

Application of the ECRH radiation for plasma diagnosis in Wendelstein 7 X

D. Moseev[1], H.P. Laqua[1], S. Marsen[1], T. Stange[1], I. Abramovic[1,2], A. Cappa[3], H. Braune[1], F. Gellert[1,4], W. Kasparek[5], S.K. Nielsen[6], J.W. Oosterbeek[1,2], M. Salewski[6], M. Stejner[6], T. Wauters[7], M. Weissgerber[8] and Wendelstein 7-X team[1]

[1]Max-Planck-Institut für Plasmaphysik, Greifswald, Germany
[2]Eindhoven University of Technology, Eindhoven, The Netherlands
[3]National Fusion Laboratory, CIEMAT, Madrid, Spain
[4]ErnstMoritzArndt University, Greifswald, Germany
[5]University of Stuttgart, Stuttgart, Germany
[6]Technical University of Denmark, Kgs. Lyngby, Denmark
[7]Laboratory for Plasma Physics, ERM/KMS, Brussels, Belgium
[8]Max-Planck-Institut für Plasmaphysik, Garching, Germany

Corresponding Author: dmitry.moseev@ipp.mpg.de

Abstract:

Wendelstein 7-X is an optimized stellarator with n=5 symmetry. It had its first operational phase in December 2015 - March 2016. The machine is equipped with a powerful electron cyclotron resonance heating (ECRH) system with a total power of 4.5 MW and to be doubled for the next experimental campaign. The 140 GHz ECRH radiation is used for qualitative and quantitative investigation of the plasma parameters, such as ion temperature, microwave absorption, etc. Here we concentrate on sniffer probes as a diagnostic of the microwave absorption and collective Thomson scattering (CTS) for ion temperature measurements.

1 Introduction

Wendelstein 7-X (W7-X) started its first experimental campaign OP1.1 in December 2015. The ECRH was the only heating source available and it was used for plasma start-up and wall conditionning [1]. In the beginning, the ECRH protective diagnostics, namely sniffer probes, provided important information on plasma formation. This topic is covered in Section 2.

For OP1.2 a Collective Thomson Scattering (CTS) diagnostic is planned to be installed on W7-X which is similar to the CTS diagnostic on ASDEX Upgrade [2, 3, 4, 5, 6, 7]. The CTS diagnostic has proven its capability for ion temperature measurements on several tokamaks [8, 9] and stellarators [10]. Recently a feasibility of T_i measurements by CTS, having the second harmonic electron-cyclotron resonance in direct view of the receiver,

was demonstrate on ASDEX Upgrade [11]. The prospect and design of the CTS diagnostic for W7-X is discussed in Section 3. Section 4 concludes this proceeding.

2 Sniffer probes

Wendelstein 7-X is equipped with five absolutely calibrated sniffier probes [12], one for each of five identical modules of the machine, equidistantly located around the torus. Their locations with respect to each other and ECRH launchers are shown in Fig. 1 on the left panel.

The sniffer probes have various attenuators, where attenuation grows with the proximity to the ECRH launchers in order to ensure that the microwave diodes in the sniffer probes work in the linear regime.

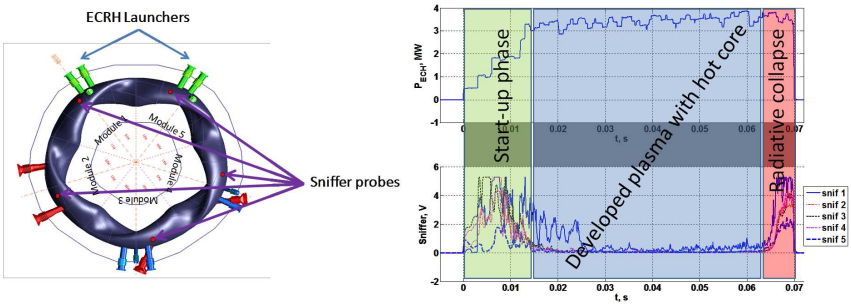

FIG. 1: Left panel: top view of the sniffer probe locations (red circles) with respect to the ECRH launchers (green ports) and each other. Right panel: time trace of total ECRH power injected into Wendelstein 7-X (15.12.2015 at 15:40 UTC); below: time traces of five sniffer probes for the same experiment. Three phases are clearly distinguishable: plasma start-up in the first milliseconds, developed plasma with the hot core, and radiative collapse due to high-Z impurities at the end. The sniffer probe interlock terminates the plasma.

In the beginning of OP1.1, a limited number of plasma diagnostics was available. Sniffer probes were used to identify the periods when the plasma had an optically thick core for 140 GHz extraordinary (X) mode microwaves with 2.52 T magnetic field on axis. Sufficient optical thickness is ensured for a plasma density of about $0.5 \cdot 10^{19}$ m^{-3} and an electron temperature higher than 300 eV. The sniffer probe signals on for an example experiment are shown on the right panel of the Fig. 1. The upper part of the panel shows a time trace of the total ECRH power being injected into W7-X as the only heating source. The lower part of the panel demonstrates five time traces of raw sniffer probe signals. Three phases are clearly seen at the sniffer signals:
(1) When ECRH has just been applied, the energy flux of stray radiation detected by all five sniffer probes is large, and some probes go into saturation. This phase is characterized by the absence of optically thick plasma for 140 GHz X-mode microwaves.
(2) Approximately 15 ms after the ECRH had started, sniffer signals decay by two orders of magnitude. In this case practically all microwave radiation emitted by the gyrotrons is absorbed. The analysis presented in reference [13] indicates that the microwave absorption coefficient of the plasma exceeds 95%.

(3) The final phase of the experiment is its termination. Due to the poor wall conditioning in the beginning of OP1.1, the cold front, due to the impurities outgassed from the wall of the vessel, propagates from the plasma edge into the center. During the process, the optical thickness of the plasma drops, and thus the microwave absorption of the plasma degrades and the sniffer signals are going up. Above a threshold the interlock based on the sniffer probes activates and switches ECRH off. A detailed overview of the ECRH safety diagnostics is presented at this conference by S. Marsen (EX/P5-13).

3 Collective Thomson Scattering (CTS)

Collective Thomson Scattering is scattering of electromagnetic waves off the collective fluctuations in the plasma. The measurements are done using the probing beam with the wave vector $\vec{k}^i$ which is scattered on fluctuations in the plasma and the receiver beam with the wave vector $\vec{k}^s$ that detects scattered wave. Salpeter [14] found, that if the following parameter $k^\delta \cdot \lambda_D \gg 1$, where $\vec{k}^\delta = \vec{k}^s - \vec{k}^i$ and λ_D is the Debye length, than the microwave scattering is collective. The CTS diagnostic measures a spectrum of scattered microwaves. Generally, the spectrum shape and magnitude depends on the scattering geometry and many of the plasma parameters: T_i, T_e, n_e, Z_eff, etc. Comprehensive models [15] exist which allow inference of the plasma parameters using forward modeling. The Bayesian inference is to be used for T_i measurements in W7-X. An example of the scattering functions (which resemble the shape of the spectra) for the O-O mode scattering and the probing frequency of 140 GHz and an electron temperature $T_e = 8$ keV, ion temperature $T_i = 4$ and $T_i = 8$ keV, magnetic field $B = 2.4$ T, electron density $n_e = 10^{20}$ m^{-3} is shown in Fig. 2. One can clearly see the influence of ion temperature on the shape of the spectrum.

One of the key geometrical parameters of CTS is projection angle $\phi = \angle(\vec{B}, \vec{k}^\delta)$. When the projection angle ϕ is close to 90°, the signature of ion cyclotron motion gets pronounced [16, 17, 8] and generally the efficiency of scattering grows. It makes isotope analysis of the plasma possible. The projection of ion velocity distribution function is also measured along the direction of $\vec{k}^\delta$, therefore by changing the projection angle, various parts of the ion velocity distribution function can be measured [18].

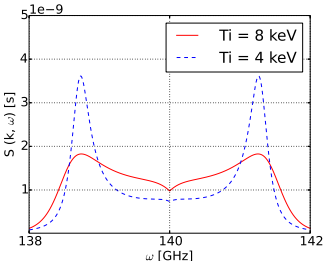

FIG. 2: Two example spectra where ion temperature is varied (4 and 8 keV), having the other parameters fixed: $T_e = 8$ keV, $B = 2.4$ T, $n_e = 10^{20}$ m^{-3}, $f_{probe} = 140$ GHz.

In OP1.2, the W7-X ECRH system will include ten gyrotrons working at 140 GHz, a quasi-optical transmission line, and several launchers located in modules 1 and 5 of the stellarator. More detailed description of the ECRH setup is given in reference [19]. The CTS diagnostic will extensively use the

ECRH infrastructure of W7-X, namely:
(1) The ECRH launcher for the gyrotron that has not been installed yet, so the launcher to be used for receiving scattering radiation.
(2) A part of the transmission line from the ECRH tower to the matching optic unit (MOU) at the end of the ECRH transmission line.
(3) A gyrotron as a source of probing radiation.

The diagnostic will be able to collect scattered microwaves from two different location. The receiving mirrors are installed in the bean-shaped cross-section of the plasma (where ECRH usually heats the plasma from) and in the trianglular cross-section. These cross-section are shown in Fig. 3. This system will use the remote steering launcher [20, 19] in order to guide probing radiation into the triangular cross-section. One gyrotron in each of two modules (modules 1 and 5) has a possibility to be connected to the remote steering launcher in the triangular cross-section in modules 1 and 5, respectively. The switching is done by means of the steerable mirror in the quasi-optical transmission line. The receiver is connected via the matching optics unit and the quasi-optical transmission line to the receiver mirrors in module 1 in the triangular and bean-shaped cross-sections. The switching between the two locations is done by the replaceable mirror in the vicinity of the launcher in the bean-shaped cross-section, in the ECRH Tower 1. The switching can be performed whenever there is an access to the torus hall, which means weekly during the campaign.

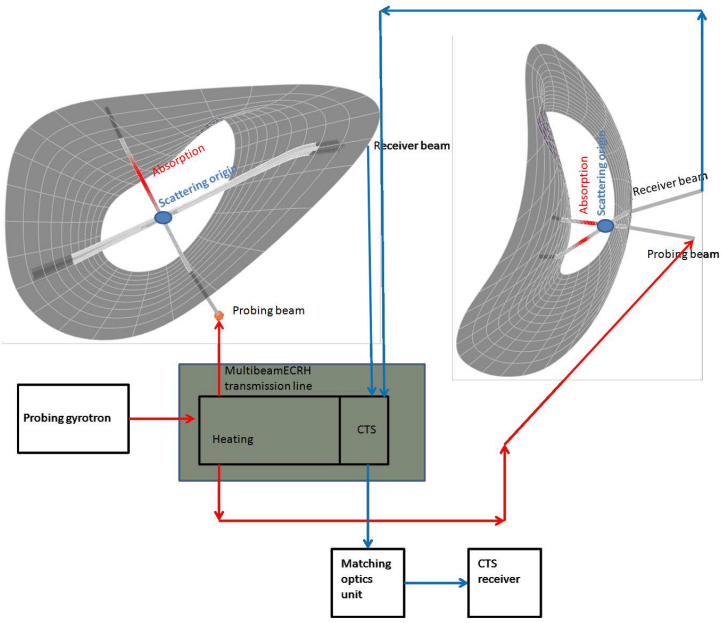

FIG. 3: The diagram of the CTS diagnostic. Two stellarator cross-sections are shown where the CTS will be measuring. On each of the cross-section, a last closed flux surface is indicated. Two beams are assigned as a probing beam and as a receiving beam on each of the cross-section. Red coloring along the beam lines in the plasma show the position of electron cyclotron absorption. The location where two beams intersect in the plasma is denoted as an origin of the measured scattering radiation. Red arrows indicate a direction of the power flow from the gyrotron (a source of probing radiation) to the plasma via multibeam quasi-optical ECRH transmission line. The blue arrows show a power flow of the scattering radiation into the CTS receiver (heterodyne radiometer) via the multibeam quasioptical ECRH transmission line and the matching optics unit.

3.1 Receiver mirror in the bean-shaped cross-section

The receiver mirror in the bean-shaped cross-section in module 1 is already installed and it is shown in Fig. 4. The mirror is steerable in two dimensions and allows scattering geometries (in combination with the mirror for the probing gyrotron) with the projection angle $\phi = \angle(\vec{B}, \vec{k}^{\delta})$ in the range of 75°- 115°. However, there is a second harmonic electron cyclotron (ECE) resonance right in the center of the plasma in this cross-section. Hence the plasma center cannot be measured by CTS because of the absorption of the probing beam. Moreover, the EC resonance layer does not only absorb, but also emits microwaves at the frequency range which is covered by the CTS receiver, 138-142 GHz which significantly decrease signal-to-noise ratio. However, recent experiments on ASDEX Upgrade [11] showed that the T_i measurements are possible and the results agree with the ion temperature obtained by the charge exchange diagnostic.

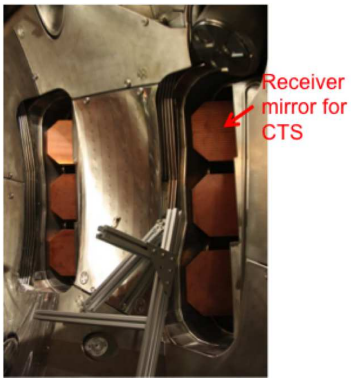

FIG. 4: A photo from inside the vacuum vessel of W7-X showing the launcher which will be used as a CTS receiving mirror in OP1.2. The mirror below it corresponds to the gyrotron launcher which will be used as a source for probing radiation.

The analysis of electron-cyclotron radiation by the TRAVIS code [21] gives the electron cyclotron emission (ECE) spectral power density for the O-mode emission around 3.5 keV, for X-mode emission approximately 1.5 keV for a core electron temperature of $T_e = 8$ keV and a core electron density $n_e = 6 \cdot 10^{19}$ m^{-3}. The Bayesian error propagation analysis [22] shows that in order to achieve the inference precision of below 10% and taking all other inference-relevant parameters as known (i.e. that the ECE noise is the only source of error), the integration time for the diagnostic should be in the order of 1 s for O-mode scattering and in the order of 100 ms for X-mode scattering.

3.2 Receiver mirror in the triangular cross-section

The second receiver system is installed in the triangular crossection of W7-X in module 1 and uses the beam from the remote steering launcher [20] as a probing source. Both beams are steerable only in one dimension and therefore the system will not be very flexible. In the plasma center it will allow a projection angle $\phi = 110°$. The 1D beam steering is adjusted in such a way that at the reference position of the probing beam, the receiver beam scans along it. The steering planes of the receiver and the probe are intersecting. Fig. 5 shows a setup of a receiving part of the CTS diagnostic in the triangular cross-section. The left panel illustrates the relative locations of the W7-X vessel, the port plug-in with the receiver mirror, and the transmission line between the plug-in and the ECRH tower, where it couples into part of the ECRH quasi-optical transmission line, reserved for CTS. A closer look at the plug-in can be taken on the right panel of the figure. The radiation is transferred as a Gaussian beam by a series of copper mirrors. At the

end of the plug-in the received radiation is transferred through the vacuum interface (a quartz window) into the only movable mirror in the installation. By means of this mirror, a direction where the receiver beam originates from, can be chosen.

The advantage of this port configuration is the absence of the EC resonance in the direct view of the receiver due to the non-axisymmetric magnetic field in W7-X. However, the reflections of the ECE at the receiver frequencies may enter the receiver via reflections from the walls. In order to account for it, a simplified model of the W7-X vacuum vessel is used in TRAVIS ECE calculations. The walls are considered perfectly reflective and the polarization of the EC wave does not change polarization after reflection. Therefore the amount of EC radiation entering the receiver is overestimated by the code. The spectral power density of ECE entering the receiver is around 300 eV and 2 keV for O- and X-mode, respectively, for the central $T_e = 8$ keV and $n_e = 6 \cdot 10^{19}$ m^{-3}. The integration time in order to achieve relative error in T_i inference below 10% is around 10 ms and 300 ms for the O- and X-mode receiver polarizers settings, respectively.

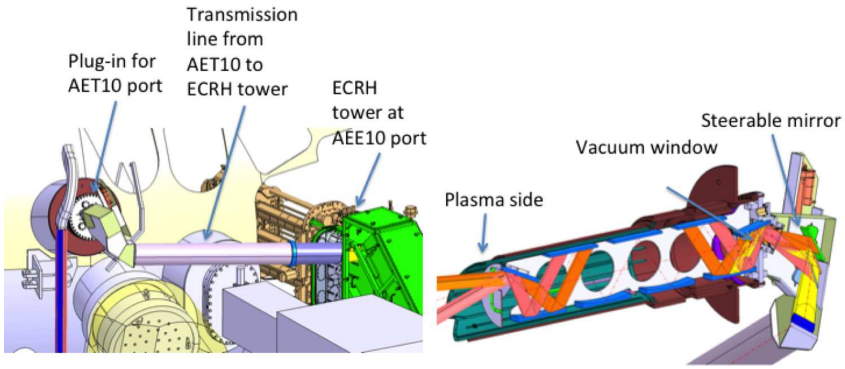

FIG. 5: A blueprint illustrating the installation of the CTS diagnostic in the port in the triangular cross-section. The port plug-in with the receiver mirror and the transmission line from the port to the ECRH tower, where it is coupled into the ECRH transmission line, is shown in the left panel. The right panel depicts a zoomed view on the plug-in for the CTS receiver port in the triangular cross-section. The radiation is transmitted quasi-optically via a series of copper mirrors. The only moving mirror is located outside of the vacuum vessel.

3.3 CTS Receiver

The CTS receiver at W7-X, a heterodyne radiometer, will be installed in the gyrotron cage outside of the torus hall and the ECRH transmission line. The receiver will be equipped with 10 channel filter bank covering a frequency range 138-142 GHz for commissioning, and a fast ADC from National Instruments with a sampling rate of 12 Gsamples per second and bandwidth of 5 GHz. The design of the receiver is similar to the one used at ASDEX Upgrade [9, 4]. The receiver will be equipped with an active voltage-controlled attenuator in order to prevent damages of the mixer in case of the reflected gyrotron power or increased level of stray radiation due to the lost mode of one of the heating gyrotrons.

4 Conclusions

Sniffer probes proved to be a reliable first line security diagnostic which additionally provides a quantitative information on microwave absorption coefficient of the plasma. It can reliably diagnose poor microwave absorption, therefore an interlock for the machine protection.
Collective Thomson Scattering is designed to measure ion temperature in the plasma core of Wendelstein 7-X. Despite high ECE background level, 10% accuracy can be achieved with 10-300 ms averaging of the scattering spectrum, depending on the receiver launcher location, plasma parameters, and polarization. The diagnostic will have two receiver locations which allows a variety of scattering geometries and accessible radial locations in the plasma.

Acknowledgments

This work has been carried out within the framework of the EUROfusion Consortium and has received funding from the Euratom research and training programme 2014-2018 under grant agreement No 633053. The views and opinions expressed herein do not necessarily reflect those of the European Commission.

References

[1] T Wauters et al. In *43rd EPS Conference on Plasma Physics*, page P4.047, Leuwen, Belgium, 2016.

[2] F Meo et al. *The Review of scientific instruments*, 79(10):10E501, 2008.

[3] M Salewski et al. *Nuclear Fusion*, 50(3):035012, 2010.

[4] V Furtula et al. *Review of Scientific Instruments*, 83(1):013507, 2012.

[5] J Rasmussen et al. *Plasma Physics and Controlled Fusion*, 57(7):075014, 2015.

[6] S K Nielsen et al. *Plasma Physics and Controlled Fusion*, 57(3):035009, 2015.

[7] M Stejner et al. *Plasma Physics and Controlled Fusion*, 57(6):062001, 2015.

[8] M Stejner et al. *Plasma Physics and Controlled Fusion*, 55(8):085002, 2013.

[9] M Stejner et al. *The Review of scientific instruments*, 85(9):093504, 2014.

[10] M Nishiura et al. *Nuclear Fusion*, 54(2):023006, 2014.

[11] M Stejner et al. *submitted to Plasma Physics and Controlled Fusion*, 2016.

[12] D Moseev et al. *Review of Scientific Instruments*, 87(8):083505, 2016.

[13] D Moseev et al. *submitted to Nuclear Fusion*, 2016.

[14] E E Salpeter. *Physical Review*, 120(3):1528, 1960.

[15] H Bindslev. *Journal of Atmospheric and Terrestrial Physics*, 58(8):983–989, 1996.

[16] S B Korsholm et al. *Physical Review Letters*, 106(16):165004, 2011.

[17] M Stejner et al. *Plasma Physics and Controlled Fusion*, 54(1):015008, 2012.

[18] M Salewski et al. *Nuclear Fusion*, 51(8):083014, 2011.

[19] V Erckmann et al. *Fusion Science and Technology*, 52(2):291–312, 2007.

[20] V Erckmann et al. In *Fusion Energy 2006*, pages IT/2–4Rd, Chengdu, 2007. International Atomic Energy Agency.

[21] N B Marushchenko et al. *Computer Physics Communications*, 185(1):165–176, 2014.

[22] M Stejner et al. *Nuclear Fusion*, 52(2):023011, 2012.